Investigation of Distress in the South Tower of the Milwaukee City Hall

By Steven DelloRusso, P.E., Brent Gabby, P.E. and Donald Dusenberry, P.E.

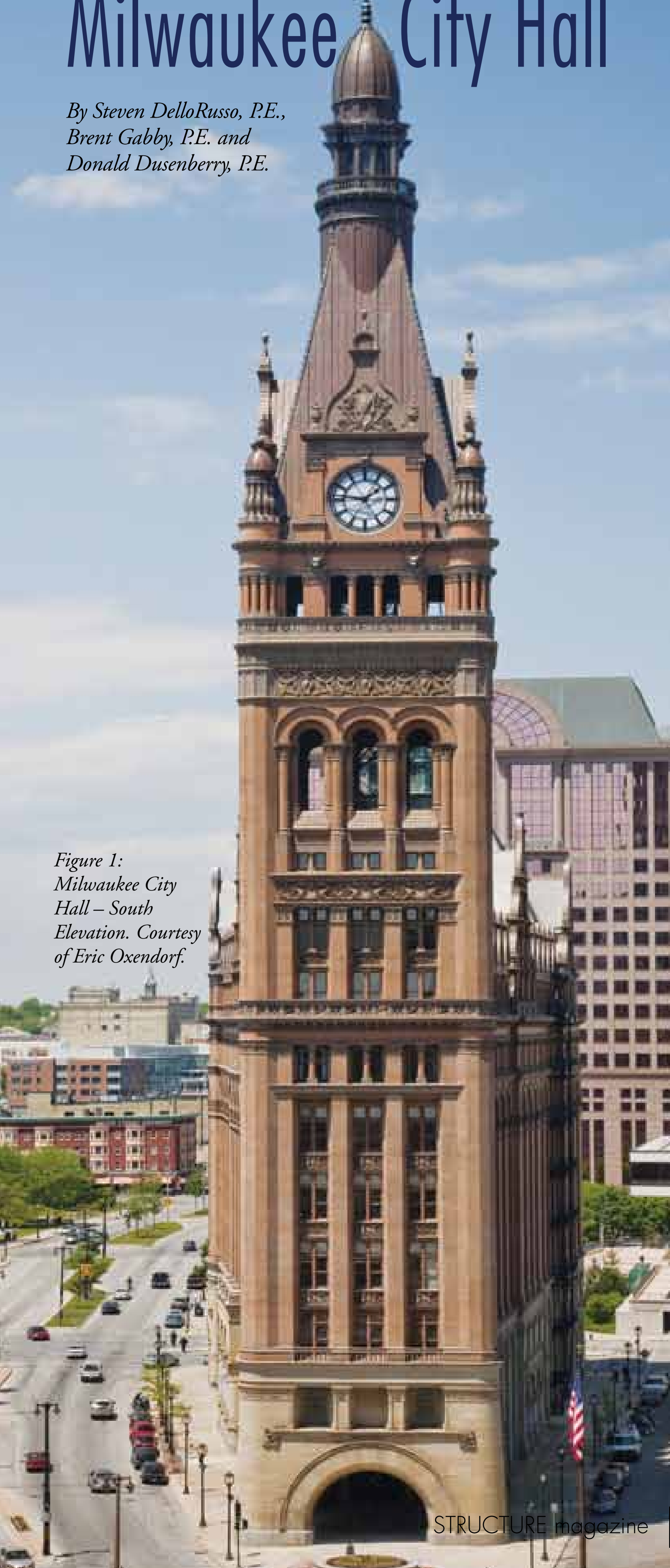

Figure 1: Milwaukee City Hall – South Elevation. Courtesy of Eric Oxendorf.

THE MILWAUKEE CITY HALL, a National Historic Landmark, was built between 1893 and 1896. Designed in the German Renaissance Revival style by Henry C. Koch & Co., the building is situated east of the Milwaukee River and has three distinctive features: the 390-foot South Tower with a copper spire and lantern, a 235-foot copper clad North Tower, and the mansard and hipped slate roofs on the nine-story main building connecting the two towers. The building, a perimeter-load-bearing masonry structure supported on wood piles, is trapezoidal in plan and approximately 300-feet long. The largely brick masonry exterior walls contain decorative terra cotta, sandstone, and granite elements with repetitive massing and detailing throughout (*Figure 1*).

Starting as early as 1909 and continuing through the 1970s, the City of Milwaukee has embarked on several major repair campaigns to address distress in the building. In 2001, the City once again decided to investigate the continuing distress, and retained Simpson Gumpertz & Heger Inc. to inspect the building and recommend repairs and cost estimates for a durable long-term solution.

This article, which describes the investigation, is the first in a three-part series about the eight-year effort to assess and analyze the South Tower, design repairs above the eleventh floor, and monitor construction. Subsequent articles will describe the solutions to the structural and building envelope deficiencies of the South Tower.

The South Tower Structure

The upper portion of the South Tower is a hybrid steel and masonry structure, approximately 56 feet square in plan, consisting of masonry perimeter walls up to 54-inch thick and a central four-sided steel truss (the core truss) that extends vertically from the ninth floor to the top of the roof spire (*Figure 2*). At the ninth floor, the core truss is supported on two built-up steel trusses that span diagonally between opposite tower corners.

The thirteenth floor has 18-foot diameter clock faces on gables on all four elevations. Ornamental masonry turrets are located in the corners at the base of the roof. Above the thirteenth floor, the core truss, which is roughly 12 feet square in plan, is stiffened by additional triangular steel roof trusses that extend from the core truss to plate girders embedded in the masonry walls supporting the thirteenth floor. The trusses are restrained by tension rods that extend downward to the tenth-floor level. The roof trusses form the slope of the roof.

The spire roof is supported by the roof trusses and the masonry perimeter walls. Structural tee purlins span between the roof trusses and support terra cotta tile, which form the roof deck below the copper roof. A spiral steel staircase located within the core truss provides access to the upper levels and lantern.

All floors above floor nine are unheated and the masonry arches on floors ten and twelve are open, leaving the interior of the tower exposed to ambient conditions.

Field Observations

Staging the structure for the investigation was impractical. Therefore, we used industrial rope access techniques to inspect the main façade, sloped roofs, and exterior ornamental features, including large turrets, finials, and arches (*Figure 2*). This inspection revealed extensive masonry cracking and deterioration that was not easily detected by ground or interior observation.

Masonry Cracking

The masonry walls and ornamental terra cotta elements had numerous cracks. Although some distress was local in nature and did not relate to overall structural behavior of the tower, many of the cracks were very large and suggested overall deficiencies in the structural performance of the South Tower. In addition, many of the largest cracks had been repaired previously and subsequently reformed or propagated. This continuing damage indicated that the cracking was active and that the previous repairs had not addressed the underlying causes.

Some of the significant cracking extended from the masonry arches on floor ten upward into the brick walls of floor eleven (*Figure 3*). In addition, significant gaps were between the exterior masonry walls and the flooring systems on floors eleven and twelve. These gaps suggested that the tower was spreading in response to loads and environmental conditions. Circular columns at floor twelve had large vertical cracks, indicating that the columns were splitting.

Corrosion, Deterioration of the Roof Elements – Effects of Water Intrusion

The copper spire, installed in 1923 to replace the original slate roof, was worn thin and open in many locations. The terra cotta tile forming the roof deck contained heavy efflorescence. Tile was so deteriorated in some locations that both small and large pieces of the tiles were falling onto the thirteenth floor, prompting the City to declare floor thirteen a hard hat zone.

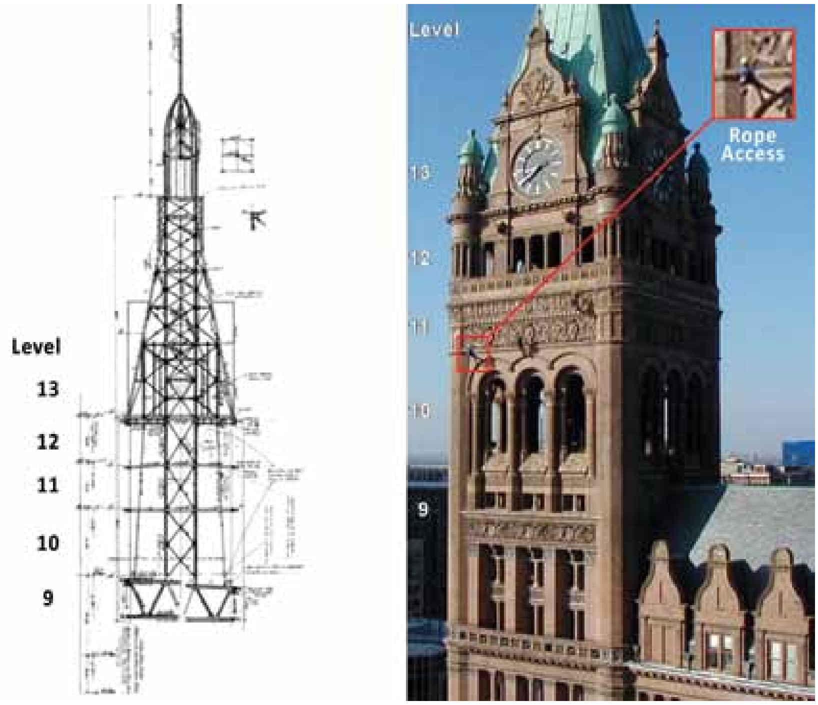

Figure 2: South Tower Structure.

In general, the structural steel framing not embedded in masonry was coated to protect it from corrosion. However, some of the connections in the central steel core truss at floors eleven, twelve, and thirteen had serious corrosion, including substantial build-up of corrosion product that bent connecting plates. Similarly, corrosion product build-up at the steel perimeter floor beams likely contributed to the observed gaps at floor eleven and floor twelve.

Above the thirteenth floor, we noted corrosion at framing-to-masonry interfaces, at some connections in the frame around the core truss, at the base of the lantern, and above windows in the lantern. We observed cracked and spalled masonry above the clock faces and on the clock gables where steel elements that support the main roof terminate by extending into masonry pilasters near the floor at floor thirteen. At the north gable the distress was particularly severe, resulting in a large crack, sliding of the masonry above the crack, and tilting of the adjacent turret. Working with a contractor, we stabilized the turret in place during our investigation to mitigate the potential hazard. A likely contributor to some of the observed cracks and spalls was severe corrosion of the embedded steel framing.

Structural Monitoring

In order to investigate the stability of the observed cracks, we instrumented some of them with vibrating wire crackmeters to monitor the crack width for changes over time. These crackmeters also had integral temperature sensors to facilitate correlation between crack width and ambient temperature. We installed crackmeters spanning selected existing cracks above masonry arches on floor ten (*Figure 3*), in the interior wythe of floor eleven, and above flat–topped openings on floor twelve. Crackmeter locations included different elevations, and both interior and exterior faces to monitor different exposure conditions. Additionally, we installed three sets of four thermocouple temperature sensors positioned at various depths through the thickness of the solid masonry wall to measure the thermal gradient through the wall. Two sets were located on floor ten, where the total thickness of the masonry wall is approximately 54 inches, one on the east elevation and one on the south elevation. The third set was installed on the north elevation of floor twelve where the thickness of the wall is approximately 24 inches. Lastly, we installed two strain gages on the steel framing, one at a steel tie on floor eleven and the other on a vertical member on floor thirteen. All sensors were connected to a datalogger mounted inside floor eleven. The datalogger was outfitted with a cellular telephone connection for remote access and data retrieval. We recorded data over a 14-month period.

Crackmeter measurements recorded daily cyclic movements as well as annual excursions, indicating that cracks were active and responded to temperature changes and thermal gradients through the wall thickness. Crackmeters on the exterior façade recorded greater movements than those on interior surfaces. Thermocouple data indicated thermal gradients within the thickness of the masonry, with temperature changes in the central portion of the wall lagging those near the faces. These transient gradients induce bending stresses in the stone (*Figure 4, page 24*).

We ran a theoretical 2D heat flow analysis of the masonry using weather data from the National Climatic Data Center, including the effects of historical solar radiation and temperature, for a two-week period. The theoretical trace of internal temperature of the masonry at 6 inches below the surface showed very good correlation to our thermocouple measurements at that depth on the east elevation.

continued on next page


Figure 3: Crackmeter and Thermocouple Wiring Above Floor 10 Arch.

The strain gages on the steel members indicated that thermally induced stresses caused the greatest variation, with minimal changes in stress levels from externally applied forces.

Structural Analysis

Concurrent with our field investigation, we performed finite element (FE) analyses of the tower structure and masonry components. These analyses included: a model of the steel structure, a FE model of a section of the masonry wall, and a detailed FE model of a masonry column.

Field samples extracted from the structural steel confirmed material properties for our analytical models. Brick and masonry properties used for analysis were based on test data from a previous investigation of the structure and a literature search for accepted values for materials of this building's vintage.

Our analysis showed that stress in the steel structure was within allowable levels for typical operating loads, including gravity and wind.

We modeled the masonry wall from floor nine through floor thirteen under gravity and thermal loading conditions. Results for gravity loads alone showed stresses in some locations greater than the accepted values of tensile strength of the masonry, indicating that the cracks probably formed originally under gravity loads. The locations of high stress were at the tops of the floor ten and floor twelve arches, where we observed the most significant cracking in the field (*Figure 5*). We repeated our analysis, incorporating some discontinuities in the model to represent cracks at the locations of high stress. This analysis showed that the cracks were likely to propagate under gravity loads. Unrestrained uniform temperature changes produced little changes in resulting stresses for both models.

We also modeled a horizontal section through the masonry walls at floor ten (54-inch thickness) and applied a thermal gradient consistent with the field measured gradient. The results produced stresses in the exterior face greater than the typical tensile stress. In addition, we modeled the cracks in the exterior face and reran the analysis. Results indicated that the cracks would likely continue to propagate through the thickness.

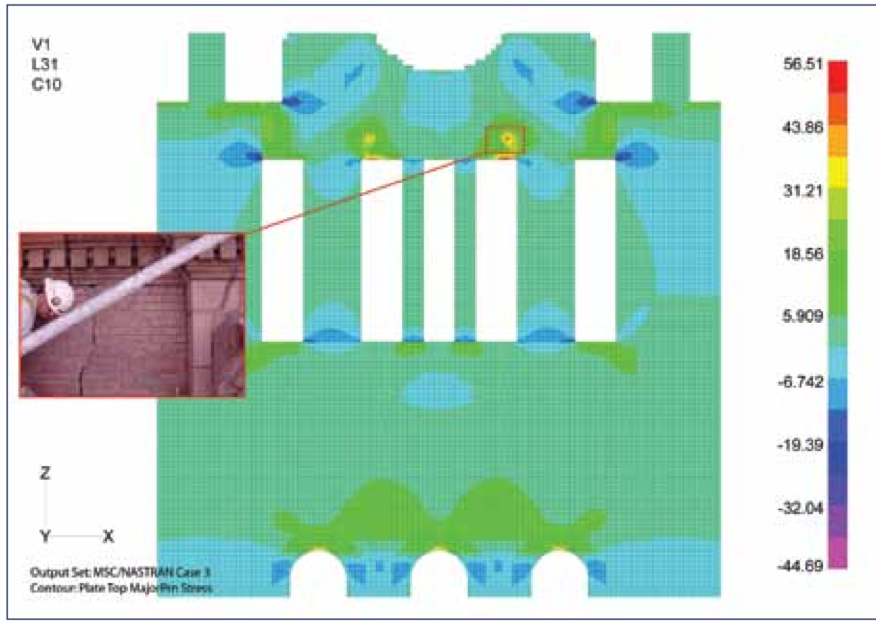

Figure 5: FEM results for Gravity Loads. Note Area of High Stress Corresponds to Location of Observed Crack on Structure.

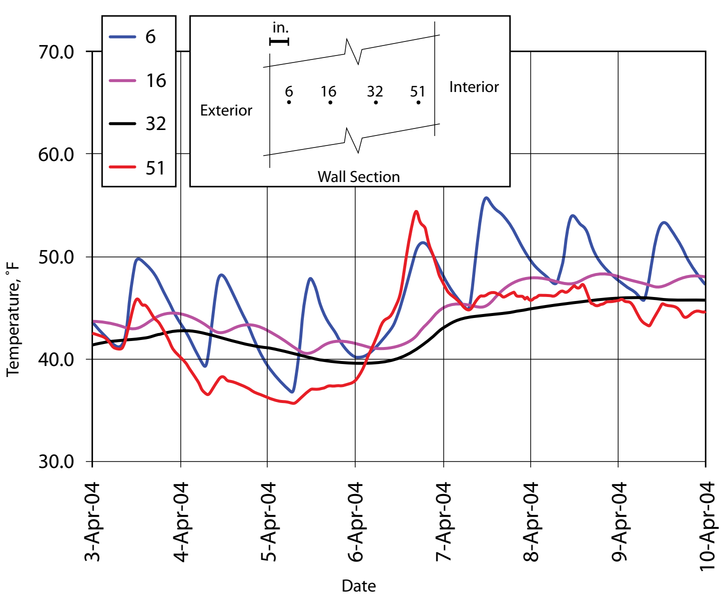

Figure 4: Daily Thermocouple Data Showing the Lag of the Central Temperatures. (East elevation – Floor 10)

We investigated thermal effects on the floor twelve masonry columns by modeling a horizontal section of one 20-inch-diameter column. The column was made with seven face bricks with a rounded surface forming an interior septagon filled with common brick. Historical test data indicated the inner brick has significantly higher moisture expansiveness than the outer brick. We assumed a slightly higher coefficient of thermal expansion for the inner brick than for the face brick, and analyzed the effects of a uniform temperature increase of 40 degrees F. Results from this model indicated that the circumferential stresses from the expansion were sufficient to initiate vertical cracks in the joints of the exterior face brick. These cracks would allow increased moisture in the inner bricks contributing to further expansion of the inner core and opening of wider cracks in the face brick.

Conclusion

Our field inspection, structural monitoring, and theoretical analysis revealed that the effects of self weight, moisture, and temperature had significantly distressed the structural system of the South Tower. Exposure, corrosion of embedded steel elements, and stresses from fundamental loads, like gravity, had caused extensive cracking of the unreinforced masonry which was the basic fabric of the Tower's structural system. Structural monitoring for more than a year demonstrated that existing cracks were active, causing further deterioration with continued exposure, creating loose masonry and increased risk of hazards from falling debris. Global and sweeping repairs would be needed to arrest the mechanisms causing distress, make the structure safe, and restore the tower to its former glory.▪

*Steven DelloRusso, P.E., is a Senior Staff II – Structures at Simpson Gumpertz & Heger Inc. He can be reached at **sjdellorusso@sgh.com**.*

*Brent Gabby, P.E., is a Senior Principal at Simpson Gumpertz & Heger Inc. He can be reached at **bagabby@sgh.com**.*

*Donald Dusenberry, P.E., is a Senior Principal at Simpson Gumpertz & Heger Inc. He can be reached at **dodusenberry@sgh.com**.*

Photos courtesy of Simpson Gumpertz & Heger Inc.